

1. Supplementary material

1.1. Sample selection



Figure S1 Sample E70

Figure S2 Sample E80

Figure S3 Sample E90

After the samples were collected, granulometry was made with the electric vibrator and the sieve assembly to obtain the granulometry fractions showed in Figure S4 and Figure S5 respectively.



Figure S4. Assembly electric vibrator and sieves.



Figure S5. Gravimetry fractions.

1.2. Optical microscopy and scanning electron microscopy

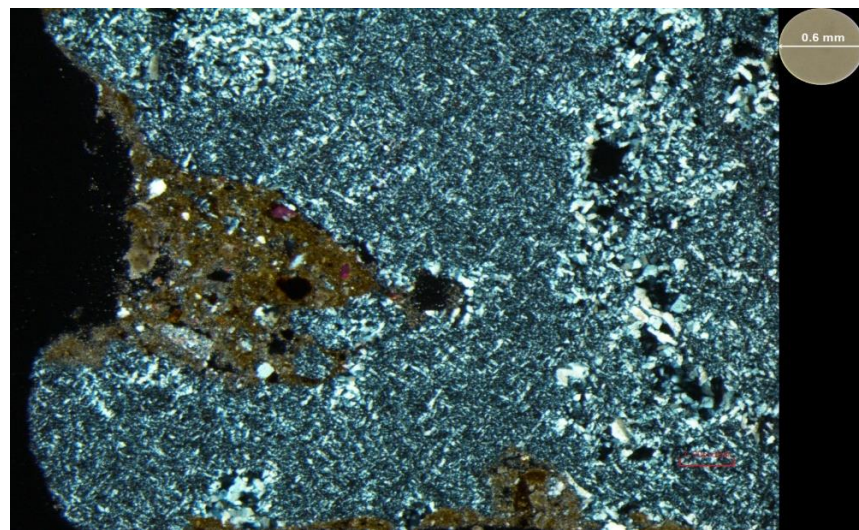


Figure S6. Optical microscopy of celestine crystals replacing carbonate, sample E69.

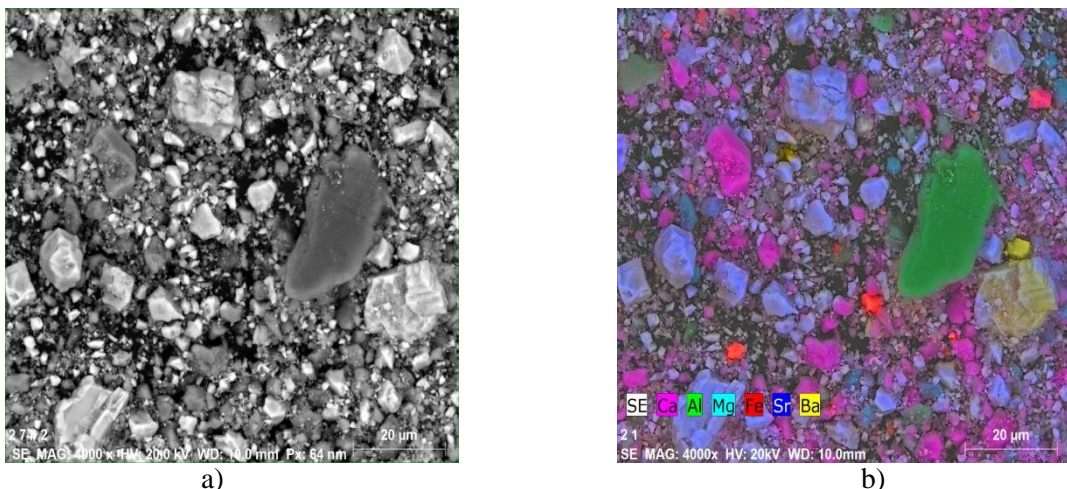


Figure S7. Scanning electron microscopy (a) and compositional SEM map of E69 sample (b).

1.3. Granulometry study

Table 1 and Figure S8 shows the % mass_r (retained mass percentage accumulated in each sieve) and f_i (the retained mass in each sieve divided between the total mass). The mass mineral above 10 mm is 12,07 % in E60 sample and the predominant fraction is 5mm-10mm. In contrast, fraction mineral >10 mm is 29,08 % in E69 and 32,52% in E92 and fraction mineral >10 mm is the predominant fraction in both cases. The 90% of mineral mass is above 315 micras in E60 and E69 samples but is above of 100 micras in E92 sample.

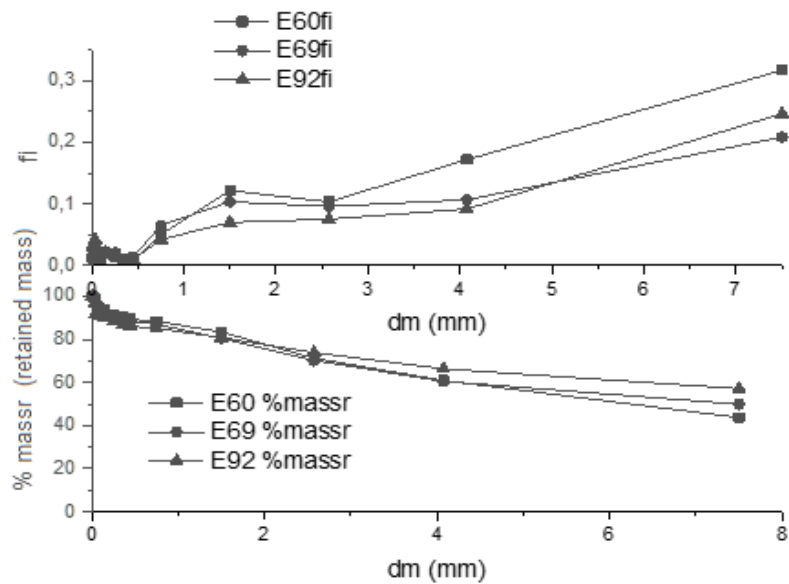


Figure S8. Granulometry results, % mass_r and f_i to each diameter (mm) in E60, E69, E92 samples.

Table S1 Granulometry results, % mass_r and f_i to each diameter (mm) in E60, E69, E92 samples.

d_m (mm)	f_i	E60		E69		E92	
		%mass _r	f_i	%mass _r	f_i	%mass _r	
>10mm	0	0,121		12,07	0,290	29,08	0,325
10mm-5mm	7,5000	0,317		43,77	0,208	49,93	0,247
5mm-	4,0750	0,172		60,95	0,107	60,60	0,092
3,15mm							66,36
3,15mm-	2,5750	0,103		71,28	0,096	70,18	0,075
2mm							73,89
2mm-1mm	1,5000	0,122		83,43	0,103	80,52	0,070
1mm-	0,7500	0,050		88,40	0,065	87,04	0,042
500μm							85,11
500μm-	0,4500	0,009		89,30	0,014	88,42	0,010
400μm							86,11
400μm-	0,3575	0,008		90,12	0,011	89,51	0,008
315μm							86,90
315μm-	0,2575	0,015		91,57	0,021	91,58	0,015
200μm							88,35
200μm-	0,1500	0,020		93,57	0,022	93,82	0,020
100μm							90,38
100μm-	0,0855	0,011		94,64	0,009	94,73	0,010
71μm							91,40
71μm-	0,0605	0,010		95,65	0,010	95,71	0,014
50μMm							92,77
50μm-20μm	0,0350	0,032		98,81	0,031	98,83	0,042
<20μm	0,0100	0,012		100,00	0,012	100,00	0,031
							100,00

This table include the E60, E69, E92 granulometric results

1.4. X-Ray fluorescence and diffraction

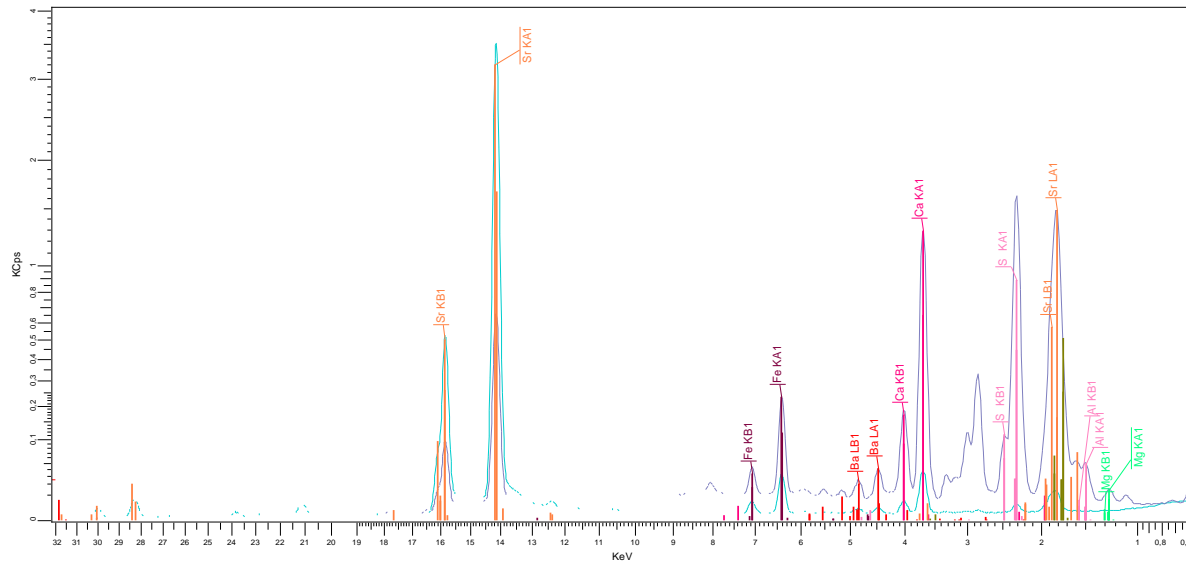


Figure S9. X-ray fluorescence (representative XRF spectra of one of the samples (E69).

1.4.1. X-Ray fluorescence and diffraction

Figure S10 shows the relationship between % Al_2O_3 and % SiO_2 obtained in XRF (Table 2).

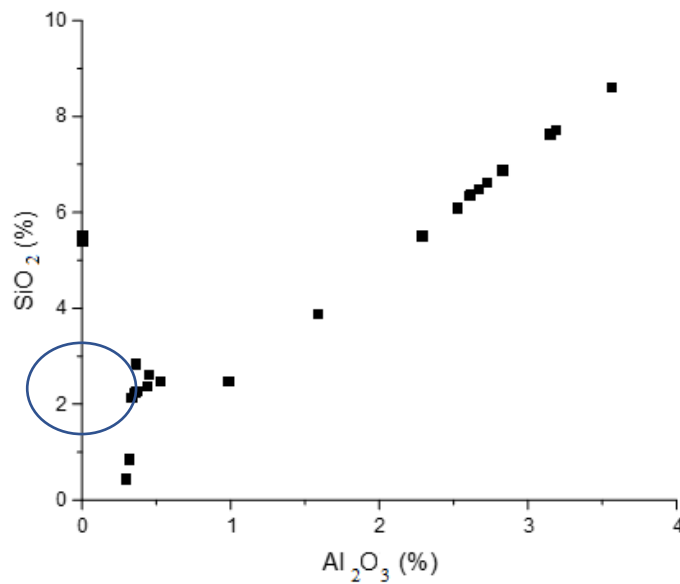


Figure S10. Correlation $\text{Al}_2\text{O}_3 / \text{SiO}_2$ obtained in XRF.

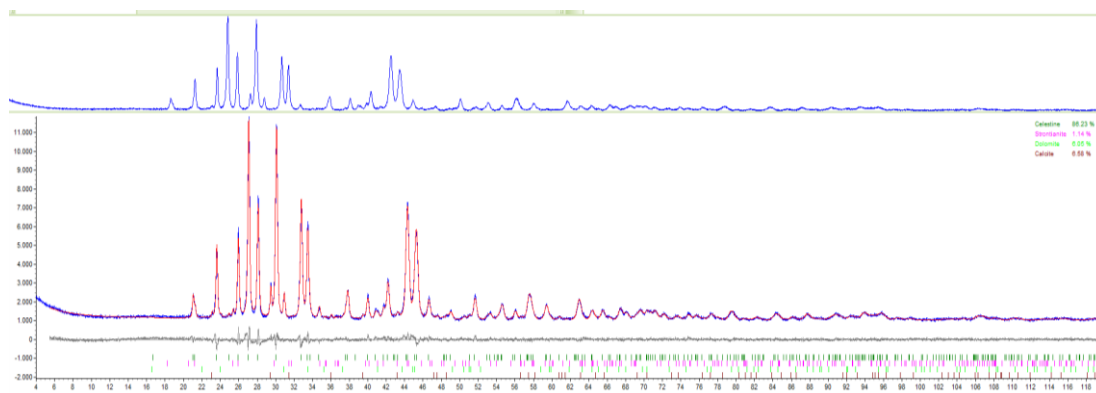


Figure S11. Rietveld refinement of X-ray diffraction data used for quantitative mineral analysis.

1.4.2. Study of XRF and DRX correlation

Figure S10 shows the relationship between % Al₂O₃ and %SiO₂ obtained in XRF (Table 2).

Data in Table 2 and Table 4 helped to make the correlation graphics of linear regression (Figure S11, S12). Figure S11 shows the relationship between % SrSO₄(Ba) obtained in XRF and DRX techniques, with a lineal fit whose equation is $y= 25,770+1,239 x$. Figure S12 shows the relationship between %CaCO₃ obtained by XRF and DRX with a lineal fit equation $y= 0,207+1,239 x$. The Pearson coefficient showed a high correlation in both mineral phases (Pearson's up to 0,98).

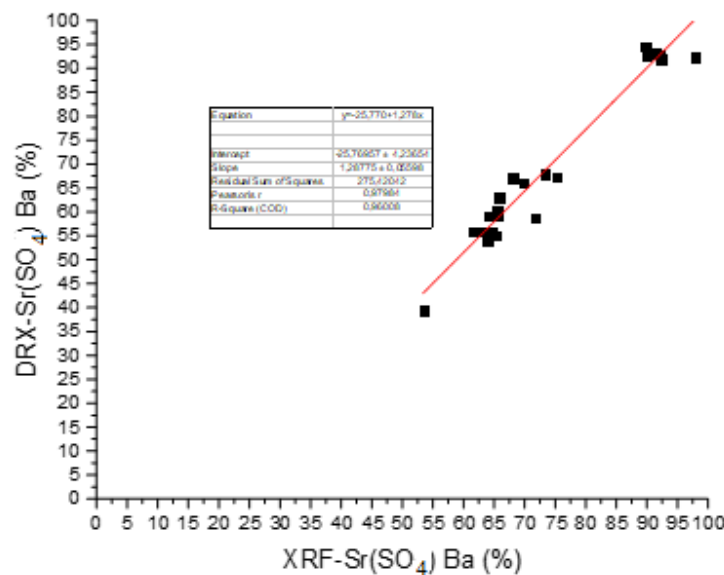


Figure S12. Linear regression model between % Sr(SO₄)Ba obtained by XRF and DRX.

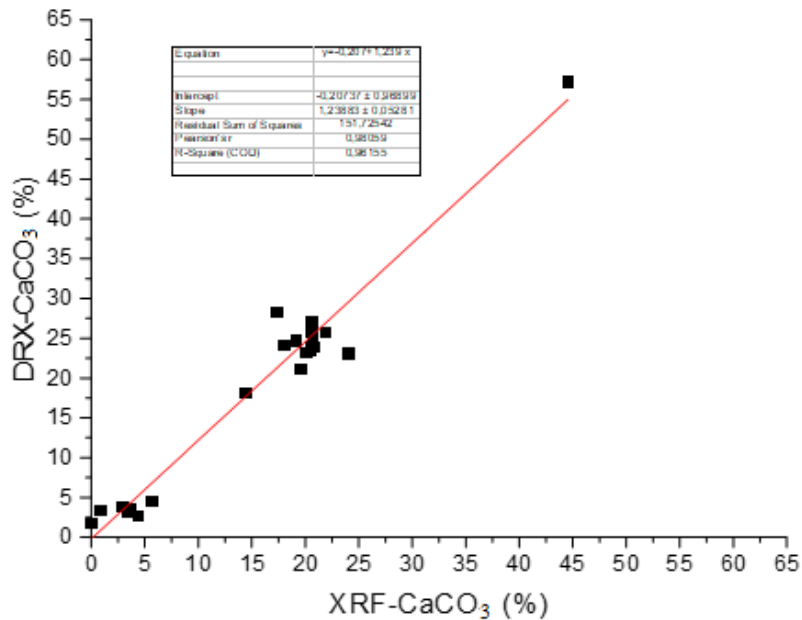


Figure S13. Linear regression model between % CaCO₃ obtained by XRF and DRX.

To validate mineralogical CaCO₃ composition by XRF and DRX results, investigators applied TGA technique.

Table S2 shows the comparison between percentage CaCO₃ by XRF and DRX with percentage CaCO₃ by TGA/DCS.

Table S2 Comparative % CaCO₃ by DRX, XRF and TGA methods

Sample	CaCO ₃ % -XR	CaCO ₃ - DRX	CaCO ₃ - TGA
E60	20,62	24,35	27,06
E60_1	20,59	27,06	26,74
E60_2	20,60	27,3	26,23
E60_3	20,07	23,33	26,01
E60_4	20,51	23,49	25,00
E60_5	19,09	24,8	24,87
E60_6	14,43	18,28	18,60
E69	18,03	23,25	27,11
E69_1	20,55	25,89	30,49
E69_2	20,55	24,03	29,76
E69_3	20,47	23,88	28,27

E69_4	21,87	25,87	28,96
E69_5	19,54	21,3	27,14
E69_6	23,95	23,24	24,79
E70	44,55	57,29	54,45
E80	17,28	28,44	25,83
E90	0	1,81	0,43
E92	2,84	3,88	4,42
E92_1	0,86	3,56	3,51
E92_2	4,31	2,74	4,41
E92_3	3,38	3,17	3,13
E92_4	3,58	3,81	3,83
E92_5	3,33	3,21	2,73
E92_6	5,59	4,62	5,51

It can be appreciated with the slope of linear regression that if XRF technique is used 23,69% carbonates are underestimated ($y = 0,036+0,763x$). If DRX technique is applied, carbonates are underestimated in 3,78% ($y = -0,524+0,962x$).

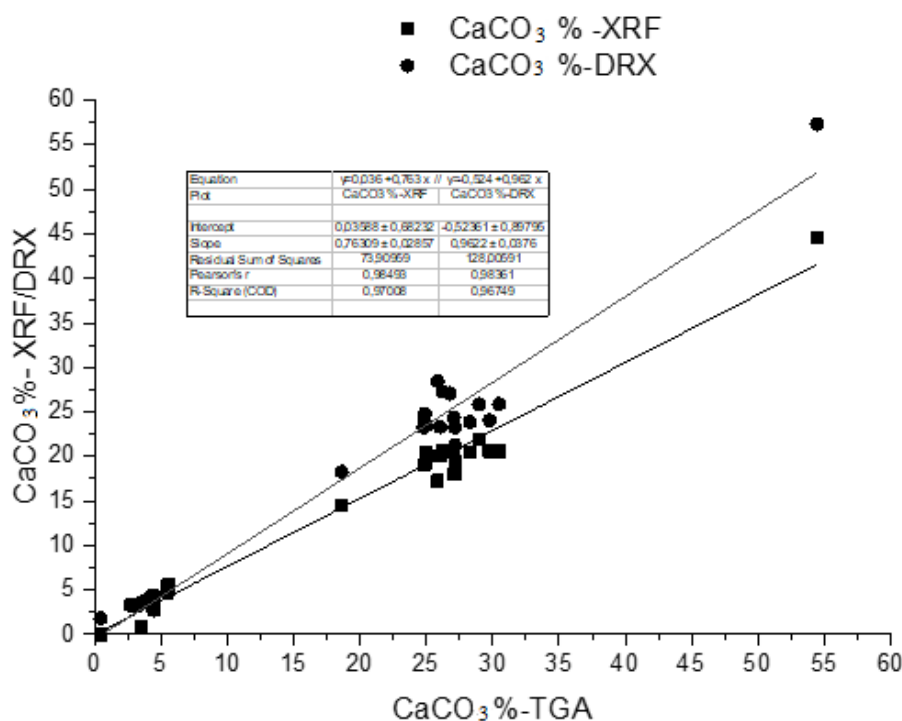


Figure S14. % CaCO₃ by TGA vs % CaCO₃ by XRF or DRX.